Inorganic Chemistry

Article

pubs.acs.org/IC

σ-Donor/Acceptor-Confused Ligands: The Case of a Chlorostibine

Iou-Sheng Ke and François P. Gabbaï*

Department of Chemistry, Texas A&M University, College Station, Texas 77843, United States

Supporting Information

ABSTRACT: In search for new examples of σ-acceptor ligands, we have investigated the tridentate ligands (*o*-(iPr$_2$P)C$_6$H$_4$)$_2$SbPh) (L^{Ph}) and (*o*-(iPr$_2$P)C$_6$H$_4$)$_2$SbCl) (L^{Cl}) which react with (tht)AuCl (tht = tetrahydrothiophene) to afford L^{Ph}AuCl (**1**) and L^{Cl}AuCl (**2**), respectively. As suggested by the structure of these complexes, which confirm complexation of the SbP_2 ligands to the gold chloride fragment, and in agreement with the results of the density functional theory (DFT) and natural bond orbital (NBO) calculations, the gold and antimony atom of **1** and **2** are involved in a Au→Sb donor−acceptor interaction. The magnitude of this interaction is higher in complex **2** which possesses a chlorinated and thus more Lewis acidic antimony center. We have also compared the strength of the Au→Sb interaction present in **2** with the Au→Bi interaction observed in the newly prepared bismuth analogue [(*o*-(iPr$_2$P)C$_6$H$_4$)$_2$BiCl]AuCl (**3**). This comparison reveals that **2** possesses a stronger Au→Pn bond (Pn = pnictogen), an observation reconciled by invoking the greater Lewis acidity of antimony(III) halides. Finally, complexes **1** and **2** undergo a clean antimony-centered oxidation when treated with *ortho*-chloranyl. These oxidation reactions afford complexes [(*o*-(iPr$_2$P)C$_6$H$_4$)$_2$(*o*-C$_6$Cl$_4$O$_2$)SbPh]AuCl (**5**) and [(*o*-(iPr$_2$P)C$_6$H$_4$)$_2$(*o*-C$_6$Cl$_4$O$_2$)SbCl]AuCl (**6**). Structural and computational studies of **5** show that the Au→Sb bond becomes shorter and more covalent upon oxidation of the antimony atom. Although the structure of **6** has not been experimentally determined, spectroscopic and computational results show a similar effect in this complex. Complex **5** and **6** constitute rare examples of metalated six coordinate antimony compounds.

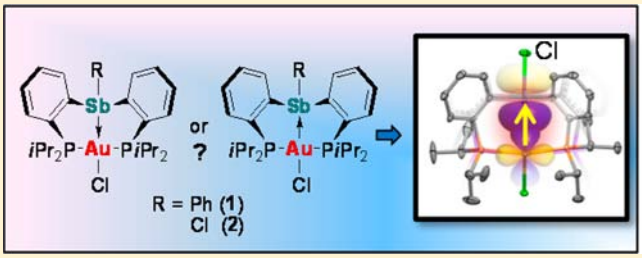

INTRODUCTION

Unlike their lighter phosphine and arsine analogues, stibine ligands tend to form relatively labile complexes when coordinated to transition metals.[1] These properties can be correlated to the moderate donicity of the antimony-based lone pair which bears a large 5s character.[2] As part of our current interest in the chemistry of such ligands, we have recently investigated the redox properties of late transition metal-stibine complexes such as **A** (Chart 1) and showed that the stibine

Chart 1

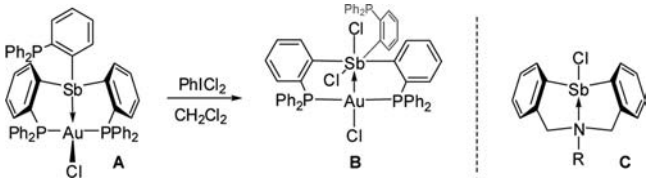

could be oxidized in the coordination sphere of the transition metal center to afford stiborane-gold complex (**B**)[2] in which the stiborane acts as a σ-acceptor.[3] This switch in the ligative behavior of the antimony ligand is accompanied by an umpolung of the Sb−Au bond from Sb→Au in the reduced state to Au→Sb in the oxidized state. An initial conclusion of these studies was that the σ-accepting properties of antimony ligand may be exclusive to the pentavalent state.[4] Recently, however, we have started to question whether such a behavior could also be observed for antimony species in the trivalent state. This revision of our thinking was prompted by the realization that antimony(III) species substituted by electronegative ligands form Lewis adducts when in the presence of Lewis basic substrates as in compound **C**.[5] An elegant contribution of Reid also demonstrated that halostibine ligands of general formula $SbMe_{3-n}Br_n$ display increased π-acceptor properties as the number of bromine atoms increases.[6] Thus, we have now decided to determine if halostibine ligands could behave as pure Lewis acidic, σ-acceptor ligands. This possibility was reinforced by the very recent discovery that chlorobismuthine ligands show Z-ligand behavior when in the coordination of electron rich metals.[7]

RESULTS AND DISCUSSION

σ-Accepting Properties of Diarylhalostibines and Comparison with Their Triaryl Analogues. To test the aforementioned hypothesis, we chose to employ a simple SbP_2 ligand system amenable to variation of one of the antimony substituents. With this objective in mind, we first targeted (*o*-(iPr$_2$P)$_2$C$_6$H$_4$)$_2$SbPh) as a triarylstibine ligand (referred to as L^{Ph}). This ligand, which was synthesized using a similar strategy as that adopted for its diphenylphosphino analogue,[4c] reacts

Received: March 26, 2013
Published: May 23, 2013

   dx.doi.org/10.1021/ic400736b | *Inorg. Chem.* 2013, 52, 7145−7151

with (tht)AuCl (tht = tetrahydrothiophene) to afford $L^{Ph}AuCl$ (**1**). Next we targeted the chlorostibine analogue of **1**. The ligand (o-(iPr$_2$P)C$_6$H$_4$)$_2$SbCl (L^{Cl}) was generated by coproportionation of neat $SbCl_3$ and (o-(iPr$_2$P)C$_6$H$_4$)$_3$Sb at 90 °C and was allowed to react, without isolation or purification, with (tht)AuCl in CH_2Cl_2 to afford $L^{Cl}AuCl$ (**2**) (Scheme 1).

Scheme 1. Reaction of L^{Ph} and L^{Cl} with (tht)AuCl

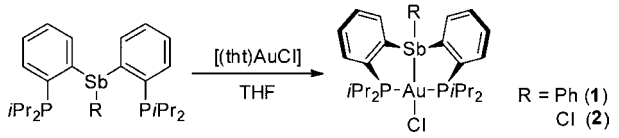

Complexes **1** and **2** are air stable and readily soluble in organic solvents such as tetrahydrofuran (THF), CH_2Cl_2, and acetone. They have been fully characterized. Their ^{31}P NMR spectra display a peak at 69.18 ppm for **1** and 64.18 ppm for **2** corresponding to the coordinated phosphine groups. These two complexes also feature a downfield ^{1}H NMR resonance at 7.92 ppm for **1** and 8.53 ppm for **2** corresponding to the phenylene proton positioned *ortho* from the antimony atom.

To gain a greater insight into the nature of these complexes, their structure has been determined using single crystal X-ray diffraction. Complex **1** crystallizes in the monoclinic space group $P2_1/c$ as a THF solvate with one molecule in the asymmetric unit (Figure 1). The coordination geometry of the

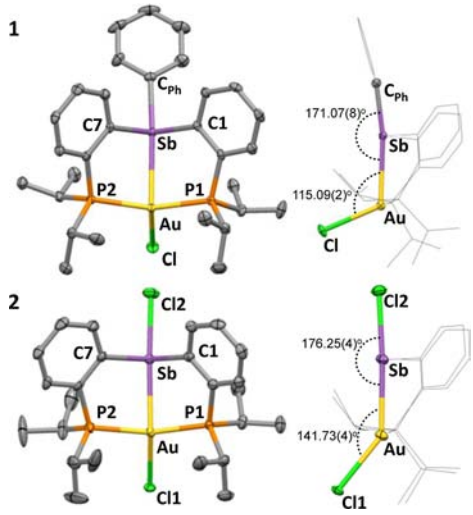

Figure 1. Structure of **1** (top) and **2** (bottom). Displacement ellipsoids are scaled to the 50% probability level. Interstitial solvent molecules and hydrogen atoms omitted for clarity. Selected bond lengths (Å) and angles (deg) for: **1**: Au−Sb 2.8669(4), Au−Cl 2.6080(8), Au−P1 2.3224(9), Au−P2 2.3244(9); P1−Au−P2 149.23(3), Cl−Au−Sb 115.09(2), Au−Sb−C$_{Ph}$ 171.07(8), C1−Sb−C7 98.28(12). **2**: Au−Sb 2.7937(13), Au−Cl1 2.5836(16), Au−P1 2.3364(19), Au−P2 2.3386(18), Sb−Cl2 2.519(2); P1−Au−P2 153.14(6), Cl1−Au−Sb 141.73(4), Au−Sb−Cl2 176.25(4), C1−Sb−C7 99.5(2).

gold atom in **1** is trigonal pyramidal, with the chloride and two phosphine ligands defining the base (P1−Au−P2 = 149.23(3)°, P1−Au−Cl1 = 104.72(3)°, P2−Au−Cl1 = 105.96(3)°; and Σ = 359.91°) and the antimony atom, the apex (Sb−Au−P1 = 84.69(2)°, Sb−Au−P2 = 84.54(2)°, Sb−Au−Cl1 = 115.09(2)°). The Au−Sb separation of 2.8669(4) Å exceeds the sum of the covalent radii of the two elements (2.64−2.75 Å) by only 4.3%−8.6%.[8] It is longer than that found in stibine gold(I) complexes including [Au(SbPh$_3$)$_4$][ClO$_4$] (2.656−2.658 Å)[9] and [Au(μ_2-1,8-(C$_{10}$H$_6$))$_2$SbPh$_2$] (2.76 Å av.).[4b] It is also slightly longer than the Au−Sb distance observed in the related complex [(o-(Ph$_2$P)C$_6$H$_4$)$_3$Sb]AuCl (2.8374(4) Å).[2] Last, with a Au−Sb−C$_{Ph}$ angle of 171.07(8)°, the stibine adopts a seesaw rather than a tetrahedral geometry. Complex **2** crystallizes in the monoclinic space group $P2_1/c$ with one molecule in the asymmetric unit (Figure 1). Although the structure of **2** resembles that of **1**, a close inspection reveals a number of notable differences. In particular, the sum of the P1−Au−P2 (153.14(6)°), P1−Au−Cl1 (105.72(6)°), and P2−Au−Cl1 (97.89(7)°) of 356.75° indicates a small but measurable displacement of the gold atom from the plane defined by the three primary ligands. The Sb−Au−Cl1 angle (141.73(4)°) is also markedly larger than the Sb−Au−Cl angle (115.09(2)°) in **1**. Altogether, these structural peculiarities suggest the presence of a Au→Sb interaction leading to a hypervalent configuration at antimony. In line with this conclusion, the Sb−Cl2 bond distance (2.519(2) Å) in **2** is intermediate between that observed for Ph$_2$SbCl (2.409 Å)[10] and [Ph$_2$SbCl$_2$]$^-$ (2.619 Å av.).[11] Also, the antimony center of **2** adopts a seesaw geometry analogous to that of [Ph$_2$SbCl$_2$]$^-$.

To shed light on the bonding present in these compounds, the structures of **1** and **2** were optimized using density functional theory (DFT) methods (Gaussian09: BP86 with 6-31g for H, C; Stuttgart relativistic small core (RSC) 1997 ECP for Au; Stuttgart relativistic large core (RLC) ECP for P, Cl, Sb) and subjected to natural bond orbital (NBO) calculations. The level of theory chosen for these calculations was first validated by a geometry optimization that produced structures very close to those determined experimentally (Table 1). For **1**,

Table 1. Selected Bond Lengths (Å) and Angles (deg) for Complexes As Determined Crystallographically (1, 2, 3, and 4) and Optimized Computationally (1*, 2*, 3*, and 4*)

	E−Au[a] (Å)	Au−Cl (Å)	P−Au−P (deg)	E−Au−Cl[a] (deg)	$\sum_\alpha$Au (deg)
1	2.8669(4)	2.6080(8)	149.23(3)	115.09(2)	379.91
1*	2.946	2.654	151.481	136.381	372.75
2	2.7937(13)	2.5836(16)	153.14(6)	141.73(4)	372.93
2*	2.845	2.636	157.877	151.632	367.69
3	2.892(2)	2.561(2)	151.96(7)	140.67(6)	373.35
3*	2.950	2.640	157.357	150.770	367.56
4	2.309(8)	2.522(2)	160.2(1)	168.7(2)	362.2
4*	2.3544	2.6486	158.48	171.23	362.36

[a]E = Sb for **1**, **2**; E = Bi for **3**; E = B for **4**.

the NBO analysis decomposes the Au−Sb interactions in two distinct components (Figure 2). The first component is a lp(Sb)→6p(Au) interaction in which the stibine ligands plays its expected role of donor toward the gold atom. The second component is a more unexpected lp(Au)→σ*(Sb−C) interaction, with the roles of the two atoms inverted. To estimate the magnitude of these interactions, we resorted to deletion calculations, which are carried out by zeroing the Kohn−Sham matrix elements corresponding to the interaction of interest. The resulting deletion energies (E_{del}(lp(Sb)→6p(Au)) = 9.4 kcal/mol and E_{del}(lp(Au)→σ*(Sb−C)) = 9.2 kcal/mol) indicate that these two interactions contribute almost equally to the stability of the complex. The opposite directionality of

dx.doi.org/10.1021/ic400736b | Inorg. Chem. 2013, 52, 7145−7151

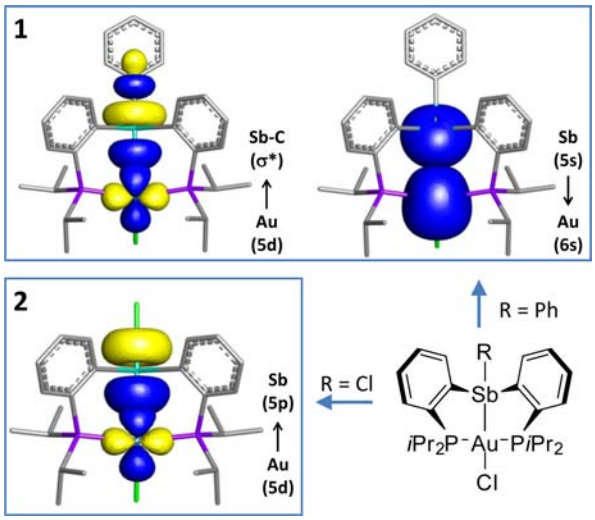

Figure 2. Superposition of the donor and acceptor NBOs for the gold-antimony interaction in **1** (above) and **2** (below). Hydrogen atoms are omitted for clarity (isovalue = 0.05).

these two interactions as well as their essentially equal contribution to the stability of the complex indicate that the gold and antimony atoms of **1** are connected by a weak (E_{del}(lp(Sb)→6p(Au) + (lp(Au)→5p(Sb)) = 18.5 kcal/mol) and nonpolar interaction.

For complex **2**, the NBO analysis treats the antimony-bound chloride as an independent unit that interacts with the antimony atom by a strong lp(Cl)→5p(Sb) interaction. This interaction may be viewed as a dative bond resulting from the donation of a chloride lone pair into a vacant antimony p orbital (Figure 2). More significantly, the same 5p orbital is involved in a 5d(Au)→5p(Sb) interaction, indicating that the gold atom donates to the antimony center by one of its filled d orbitals. A donation in the reverse direction, that is, from antimony to gold, is not observed indicating that the donor/acceptor ambiguity noted in **1** is no longer present. Hence, according to NBO, the antimony atom of **2** acts as a pure σ-acceptor or Z-ligand toward the transition metal. Finally, a deletion calculation shows that the 5d(Au)→5p(Sb) interaction stabilizes the complex by E_{del} = 24.4 kcal/mol.

Comparison of Complex 2 with Its Halobismuthine Analogue. The bonding situation observed in **1** is reminiscent of that recently described for the chlorobismuthine gold complex [(*o*-(Ph_2P)C_6H_4)$_2$BiCl]AuCl.[7] Given this relationship, we set out to determine which of antimony or bismuth would be the strongest σ-acceptor. To carry out a comparison that is exempt of phosphorus substituent effects, we have now synthesized and characterized the isopropyl derivative [(*o*-(iPr$_2$P)C_6H_4)$_2$BiCl]AuCl. This compound was prepared by reaction of the newly prepared ligand (*o*-(iPr$_2$P)C_6H_4)$_3$Bi with [(tht)AuCl] (Scheme 2). The ^{31}P NMR spectrum of the reaction mixtures shows two singlets at 57.05 ppm and 55.33 ppm integrating in a 2:1 intensity ratio (see Supporting Information). The species giving rise to a resonance at 55.33 ppm is tentatively assigned to the byproduct [{*o*-(iPr$_2$P)-C_6H_4Au}$_2$] resulting from transfer of an *o*-phenylenephosphino group from bismuth to gold. The second peak is assigned to the chlorobismuthine gold complex **3**. This assignment has been confirmed by the isolation and full characterization of **3**. Similarly to the chlorostibine analogue, this complex features a ^{1}H NMR resonance at 9.18 ppm corresponding to the phenylene proton positioned *ortho* from the bismuth atom. A single crystal X-ray diffraction analysis has also been carried out (Figure 3). Compound **3** is essentially isostructural with **2**, as

Scheme 2. Reaction of (*o*-(iPr$_2$P)C_6H_4)$_3$Bi with (tht)AuCl

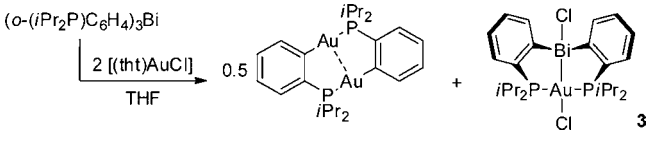

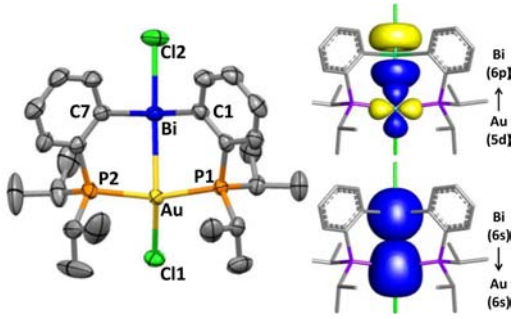

Figure 3. Left: Solid-state structure of **3**. Ellipsoids are set at 50% probability; hydrogen atoms and noncoordinated solvent molecules are omitted for clarity. Pertinent metrical parameters can be found in the text. Selected bond lengths (Å) and angles (deg) for **3**: Au−Bi 2.892(2), Au−Cl1 2.561(2), Au−P1 2.330(3), Au−P2 2.338(2), Bi−Cl2 2.613(3); P1−Au−P2 151.96(7), Cl1−Au−Bi 140.67(6), Au−Bi−Cl2 178.45(5), C1−Bi−C7 97.3(2). Right: Superposition of the donor and acceptor orbitals according to NBO analysis, which contribute mainly to the bismuth−gold interactions. Hydrogen atoms are omitted for clarity (isovalue = 0.05).

indicated by the minute differences observed in the cell parameters. This isostructural relationship is confirmed by the molecular structure of **3** and its close resemblance with that of **2**. Key metrical parameters include the Au−Bi distance (2.892(2) Å) as well as the Bi−Au−Cl1 (140.67(6)°) P1−Au−P2 (151.96(7)°), and Au−Bi−Cl2 (178.45(5)°) angles which deviate only slightly from their corresponding values in **2** (Sb−Au−Cl1 (141.73(4)°) P1−Au−P2 (153.14(6)°), and Au−Sb−Cl2 (176.25(4)°)).

For complex **3**, the NBO analysis identifies a 5d(Au)→6p(Bi) interaction which stabilizes the complex by E_{del} = 14.8 kcal/mol. A 6s(Bi)→6s(Au) is also observed. The deletion energy of this interaction (E_{del} = 5.1 kcal/mol) is however relatively low, thus indicating that it makes a minor contribution to the bonding and that the Au−Bi bond is dominated by Au→Bi character. A comparison with the results of the NBO analysis of **2** indicates that the Au→Pn interaction (Pn = Sb, Bi) is stronger in **2** than in **3**. We thus conclude that halostibines are more potent σ-acceptor ligands than their halobismuthine counterparts. This finding is in agreement with the experimentally established Lewis acidity scale which, shows that antimony(III) halides are more Lewis acidic than their bismuth(III) counterparts.[12]

Comparison of 2 with a Related Boron Analogue. Complex **2** is closely related to complex [(*o*-(iPr$_2$P)-C_6H_4)$_2$BPh]AuCl (**4**) which has been previously isolated by the group of Bourissou.[13] Complexes **2** and **4** both feature a short Au-E interaction (2.309(8) Å for E = B, 2.7937(13) Å for E =Sb) that exceeds the sum of the covalent radii (2.09−2.20 Å

dx.doi.org/10.1021/ic400736b | Inorg. Chem. 2013, 52, 7145−7151

for E = B and 2.64−2.75 Å for E = Sb) by a relatively short margin of 1.6%−5.8% in the case of **2** and 5.0%−10.5% in the case of **4**.[8] This simple metrical analysis suggests that the stabilizing energy of these linkages may be of similar magnitude. To substantiate this view, we optimized the structure of **4** using the level of theory employed for **2** and carried out a NBO analysis. As suggested by the above structural comparison, we found that the stabilization energy of the 5d(Au)→2p(B) interaction (E_{del} = 26.2 kcal/mol) of **4** only slightly exceeds that determined for the 5d(Au)→σ*(Sb−C) (E_{del} = 24.4 kcal/mol) of **2**. This comparison suggests that the ClSb of **2** and the PhB moiety of **4** have a comparable Lewis acidity toward gold, a result that we did not originally anticipate.

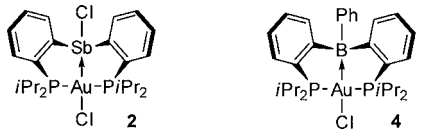

E_{del} = 24.4 kcal/mol E_{del} = 26.2 kcal/mol

Two Electron-Oxidation of Complexes 1 and 2. We have previously demonstrated that stibine gold complexes may undergo oxidation in the presence of reagents such as $PhICl_2$ to afford dichlorostiborane gold complexes with a Au→Sb interactions.[2] By analogy with such reactions, we have decided to study the oxidation of **1** and **2** in the presence of *ortho*-chloranyl, a two electron oxidant that has been previously shown to add to both triarylstibines and aryldichlorostibines.[14] To this end, these two derivatives were allowed to react with 1 equiv of *o*-chloranil in CH_2Cl_2, leading to the precipitation of complexes **5** and **6** as light orange solids (Scheme 3).

Scheme 3. Two Electron-Oxidation of Complexes 1 and 2 by *o*-chloranyl

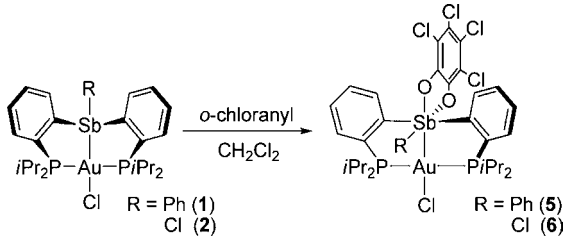

Formation of these compounds show that both **1** and **2**, despite their different binding characteristics, are amenable to a clean two-electron oxidation. The $^{31}P\{^1H\}$ NMR spectrum of **5** and **6** in $CDCl_3$ shows a single resonance at 103.26 ppm for **5** and 108.63 ppm for **6**. These resonances are significantly downfield from those of **1** and **2**, signaling a more oxidized gold atom. Complex **5** crystallizes in the rhombic space group $R\bar{3}$. The crystal structure of **5** confirms the oxidative addition of *o*-chloranil to the antimony atom which now features a tetrachlorocatecholate ligand bound in a κ^2-*O*,*O* fashion. Incorporation of this ligand leads to the formation of a six coordinate antimony atom that adopts a slightly distorted octahedral geometry (O1−Sb−Au = 162.13(8)°, C1−Sb−C7 = 172.65(15)°, C13−Sb−O2 = 173.8(2)°). This oxidative addition reaction also affects the coordination environment of the gold atom. Indeed, there is a notable contraction of the Au−Sb bond (from 2.8669(4) Å in **1** to 2.6833(3) Å for **5**) pointing to the effect of oxidation on the bimetallic core of these complexes. Also, as indicated by the value of the Sb−Au−Cl (173.91(3)°) and P−Au−P (174.09(5)°) angles, the gold atom is no longer in a trigonal pyramidal geometry but rather in a distorted square planar geometry. These changes indicate that the oxidation is not limited to the antimony atom but also affects the gold atom whose square planar geometry is consistent with a trivalent configuration.[15] Such structural changes parallel those observed upon oxidation of [(*o*-$(Ph_2P)C_6H_4)_3Sb$]AuCl with $PhICl_2$.[2] Single crystals of **6** suitable for X-ray diffraction could not be obtained, but all spectroscopic data point to a structure similar to that of **5**.

The structure of both **5** and **6** has been computationally optimized and analyzed using NBOs. The good match observed between the experimental and computed structure of **5** validates the adequacy of the level of theory employed for this complexes (Table 2). The strengthening of the Au−Sb interaction in **5** and **6** is reflected by the fact that NBO defines this linkage as a covalent one rather than as a second order donor−acceptor interaction as for **1** and **2**. Analysis of the corresponding NLMO (Figure 4) shows that the Au−Sb bonding pair possesses a larger orbital contribution from the gold atom (Sb, 16.2%/Au, 83.8% for **5** and Sb, 16.3%/Au, 83.7% for **6**) in agreement with a Au→Sb dative bond in both complexes. Changes in the NBO charges upon conversion of **1** and **2** into **5** and **6**, respectively, indicates that oxidation of the antimony atom by *o*-chloranyl also leads to a small but non-negligible increase of the charge at the gold atom (NBO charges: Au 0.447/Sb 1.101 for **1**; Au 0.453/Sb 1.008 for **2**; Au 0.451/Sb 1.897 for **5**; Au 0.467/Sb 1.815 for **6**). Finally, it is interesting to note the similarity that exists in the orbital contributions of the Au−Sb NLMOs of **5** and **6**. To explain this result, we propose that the antimony bound phenyl group (for **5**) or chloride ligand (for **6**) have little effect on the Au−Sb bond because of their *cis*-position with respect to the gold atom.

Table 2. Selected Bond Lengths (Å) and Angles (deg) for Complexes As Determined Crystallographically (5) and Optimized Computationally (5* and 6*)

	Sb−Au (Å)	Au−Cl (Å)	Sb−Au−Cl (deg)	$\sum_\alpha$Au (deg)
5	2.6833(3)	2.4886(9)	173.91(3)	360.57(1)
5*	2.780	2.600	173.298	360.689
6*	2.733	2.567	176.326	360.010

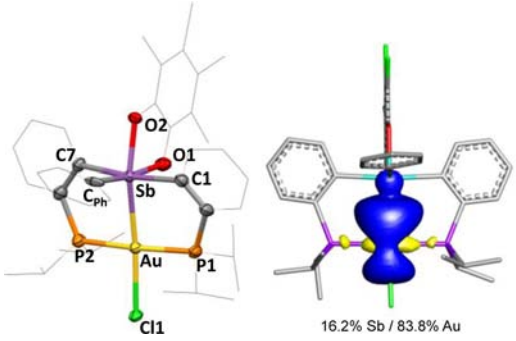

Figure 4. Left: Solid-state structure of **5**. Ellipsoids are set at 50% probability; hydrogen atoms and noncoordinated solvent molecules are omitted for clarity. Pertinent metrical parameters can be found in the text. Right: Au−Sb Natural Localized Molecular Orbital (NLMO, isovalue = 0.03). Hydrogen atoms are omitted for clarity.

dx.doi.org/10.1021/ic400736b | *Inorg. Chem.* 2013, 52, 7145−7151

CONCLUSION

The work reported in this paper shows that chlorostibine ligands, when constrained to the appropriate geometry, may behave as pure σ-acceptor ligands toward late transition metals. This possibility is illustrated by the isolation of the chlorostibine gold complex **2** which possesses a Au→Sb dative interaction. This interaction leads to an hypervalent configuration at antimony reminiscent of that found in species such as $Ph_2SbCl_2^-$, an anion formed by coordination of a chloride anion to Ph_2SbCl. The results discussed in this paper also show that the Lewis acidity of chlorostibine ligands may exceed those of analogous chlorobismuthine ligands. This conclusion is in line with the documented greater Lewis acidity of antimony(III) halides when compared to bismuth(III) halide. Finally, we show that the antimony center of gold-stibine complexes undergo a clean oxidative cycloaddition in the presence of *o*-chloranyl. This reaction, which results in the formation of a rare aurated pentavalent antimony species, is accompanied by a contraction of Au−Sb the core and a strengthening of the central Au−Sb bond.

EXPERIMENTAL SECTION

General Considerations. [(tht)AuCl][16] (tht = tetrahydrothiophene) *o*-(iPr$_2$P)C$_6$H$_4$Br[17] were prepared according to the reported procedures. Solvents were dried by passing through an alumina column (*n*-pentane and CH_2Cl_2) or by reflux under N_2 over Na/K (Et_2O and THF). All other solvents were used as received. $SbCl_3$, $BiCl_3$, and *o*-chloranyl were purchased from Aldrich and used as received. All air and moisture sensitive manipulations were carried out under an atmosphere of dry N_2 employing either a glovebox or standard Schlenk techniques. Ambient temperature NMR spectra were recorded on a Varian Unity Inova 400 FT NMR (399.59 MHz for ^{1}H, 100.45 MHz for ^{13}C, 161.74 MHz for ^{31}P) spectrometer. Chemical shifts (δ) are given in ppm and are referenced against residual solvent signals (^{1}H, ^{13}C) or external H_3PO_4(^{31}P). Elemental analyses were performed at Atlantic Microlab (Norcross, GA).

Synthesis of (*o*-(iPr$_2$P)C$_6$H$_4$)$_2$SbPh. *n*-BuLi (4.50 mL, 11.72 mmol, 2.60 M in hexane) was added into the solution of *o*-(iPr$_2$P)C$_6$H$_4$Br (2.67 g, 9.77 mmol) in Et_2O (10 mL) at room temperature. The reaction was allowed to stir for 30 min before adding solution of $PhSbCl_2$ (1.32g, 4.88 mmol) in THF (5 mL). The resulting mixture was stirred overnight at room temperature. The solvent was removed in vacuo, and the resulting solid was extracted with dichloromethane (20 mL) and filtered through Celite to remove LiCl. The filtrate was evaporated to dryness, and the residue was recrystallized from MeOH to afford (*o*-(iPr$_2$P)C$_6$H$_4$)$_2$SbPh as a white powder (1.53 g, 53% yield). ^{1}H NMR (499.43 MHz; $CDCl_3$): δ 7.44 (d, 2H, *o*-P(Sb)C$_6$H$_4$, $^3J_{H-H}$ = 7.50 Hz), 7.33 (d, 2H, SbPh−C*H*, $^3J_{H-H}$ = 7.50 Hz), 7.27 (pseudo-t, 2H, *o*-P(Sb)C$_6$H$_4$, $^3J_{H-H}$ = 7.50 Hz), 7.22 (pseudo-t, 2H, *o*-P(Sb)C$_6$H$_4$, $^3J_{H-H}$ = 7.50 Hz), 7.13−7.07 (m, 5H, *o*-P(Sb)C$_6$H$_4$ + PPh−C*H*), 2.08 (sept.d, 4H, $^3J_{H-H}$ = 4.10 Hz, $^2J_{H-P}$ = 29.03 Hz, C*H*CH$_3$), 1.07 (dd, 12H, $^3J_{H-H}$ = 3.40 Hz, $^3J_{H-P}$ = 14.51 Hz, CHC*H*$_3$), 0.80 (dd, 12H, $^3J_{H-H}$ = 3.40 Hz, $^3J_{H-P}$ = 14.51 Hz, CHC*H*$_3$). ^{13}C{^{1}H} NMR (125.58 MHz; $CDCl_3$): δ 153.72 (d, J_{C-P} = 13.82 Hz), 153.38 (d, J_{C-P} = 13.83 Hz), 143.22 (d, J_{C-P} = 8.68 Hz), 141.87 (t, J_{C-P} = 16.31 Hz), 137.31 (s), 136.75 (d, J_{C-P} = 13.84 Hz), 132.04 (s), 129.21 (s), 128.25 (s), 127.69 (s), 24.84 (dd, J_{C-P} = 13.81 Hz, J_{C-P} = 54.20 Hz), 20.22 (pseudo-t, J_{C-P} = 15.19 Hz), 19.66 (dd, J_{C-P} = 11.42 Hz, J_{C-P} = 40.21 Hz). ^{31}P{^{1}H} NMR (202.16 MHz; $CDCl_3$): δ 8.53 (s). Elemental analysis calculated (%) for $C_{30}H_{41}P_2Sb$: C, 61.56; H, 7.06. Found: C, 61.26; H, 6.97.

Synthesis of (*o*-(iPr$_2$P)C$_6$H$_4$)$_3$Sb. *n*-BuLi (3.33 mL, 8.65 mmol, 2.60 M in hexane) was added into the solution of *o*-(iPr$_2$P)C$_6$H$_4$Br (2.46 g, 7.21 mmol) in Et_2O (15 mL) at room temperature. The reaction was allowed to stir for 30 min before adding solution of $SbCl_3$ (0.55g, 2.40 mmol) in THF (5 mL). The resulting mixture was stirred overnight at room temperature. The solvent was removed in vacuo, and the resulting solid was extracted with dichloromethane (20 mL) and filtered through Celite to remove LiCl. The filtrate was evaporated to dryness, and the residue was recrystallized from MeOH to afford (*o*-(iPr$_2$P)C$_6$H$_4$)$_3$Sb as a white powder (1.39 g, 64% yield). ^{1}H NMR (399.59 MHz; $CDCl_3$): δ 7.37 (d, 3H, *o*-P(Sb)C$_6$H$_4$, $^3J_{H-H}$ = 7.72 Hz), 7.17 (pseudo-t, 3H, *m*-P(Sb)C$_6$H$_4$, $^3J_{H-H}$ = 7.72 Hz), 6.98 (pseudo-t, 3H, *m*-P(Sb)C$_6$H$_4$, $^3J_{H-H}$ = 7.72 Hz), 6.94 (d, 3H, *o*-P(Sb)C$_6$H$_4$, $^3J_{H-H}$ = 7.72 Hz), 2.02 (m, 6H, C*H*CH$_3$), 1.02 (br, 18H, CHC*H*$_3$), 0.78 (br, 18H, CHC*H*$_3$). ^{13}C{^{1}H} NMR (125.58 MHz; CDCl3): δ 155.68 (t, J_{C-P} =14.21 Hz), 143.59 (d, J_{C-P} = 10.40 Hz), 137.70 (d, J_{C-P} = 14.52 Hz), 131.54 (s), 128.67 (s), 127.10 (s), 24.74 (br), 20.28 (d, J_{C-P} = 11.97 Hz), 19.59 (br). ^{31}P{^{1}H} NMR (161.73 MHz; $CDCl_3$): δ 8.26 (s). Elemental analysis calculated (%) for $C_{36}H_{54}P_3Sb$: C, 61.64; H, 7.76. Found: C, 61.17; H, 7.80.

Synthesis of (*o*-(iPr$_2$P)C$_6$H$_4$)$_3$Bi. *n*-BuLi (6.35 mL, 18.36 mmol, 2.89 M in hexane) was added into the solution of *o*-(iPr$_2$P)C$_6$H$_4$Br (4.18 g, 15.30 mmol) in Et_2O (20 mL) at room temperature. The reaction was allowed to stir for 30 min before adding solution of $BiCl_3$ (1.61g, 5.10 mmol) in THF (10 mL). The resulting mixture was stirred overnight at room temperature. The solvent was removed in vacuo, and the resulting solid was extracted with dichloromethane (20 mL) and filtered through Celite to remove LiCl. The filtrate was evaporated to dryness, and the residue was recrystallized from MeOH to afford (*o*-(iPr$_2$P)C$_6$H$_4$)$_3$Bi as a white powder (2.33 g, 58% yield). ^{1}H NMR (499.43 MHz; $CDCl_3$): δ 7.57 (d, 3H, *o*-P(Bi)C$_6$H$_4$, $^3J_{H-H}$ = 7.85 Hz), 7.49 (d, 3H, *o*-P(Bi)C$_6$H$_4$, $^3J_{H-H}$ = 7.85 Hz), 7.26 (pseudo-t, 3H, *m*-P(Bi)C$_6$H$_4$, $^3J_{H-H}$ = 7.85 Hz), 7.11 (pseudo-t, 3H, *m*-P(Bi)C$_6$H$_4$, $^3J_{H-H}$ = 7.85 Hz), 2.07 (m, 6H, C*H*CH$_3$), 1.05 (dd, 18H, $^3J_{H-H}$ = 6.82 Hz, $^3J_{H-P}$ = 14.56 Hz, CHC*H*$_3$), 0.81 (dd, 18H, $^3J_{H-H}$ = 6.82 Hz, $^3J_{H-P}$ = 14.56 Hz, CHC*H*$_3$). ^{13}C{^{1}H} NMR (125.58 MHz; $CDCl_3$): δ 176.66 (s), 143.92 (d, J_{C-P} = 7.24 Hz), 139.75 (d, J_{C-P} = 15.78 Hz), 132.92 (s), 131.54 (s), 131.19 (s), 126.35 (s), 24.47 (d, J_{C-P} = 13.75 Hz, *C*(CH$_3$)$_2$), 20.39 (d, J_{C-P} = 17.67 Hz, CH$_{3i\text{-}Pr}$), 19.47 (d, J_{C-P} = 9.73 Hz, CH$_{3i\text{-}Pr}$). ^{31}P{^{1}H} NMR (202.16 MHz; $CDCl_3$): δ 8.68 (s). Elemental analysis calculated (%) for $C_{36}H_{54}P_3Bi$: C, 54.82; H, 6.90. Found: C, 54.52; H, 7.00.

Coproportionation of (*o*-(iPr$_2$P)C$_6$H$_4$)$_3$Sb with SbCl$_3$: Generation (*o*-(iPr$_2$P)C$_6$H$_4$)$_2$SbCl. In the absence of solvent, a 2/1 molar mixture of (*o*-(iPr$_2$P)C$_6$H$_4$)$_3$Sb and $SbCl_3$ rapidly liquefies at 90 °C, and the redistribution is complete in 3 h. The resulting (iPr$_2$P)-C$_6$H$_4$)$_2$SbCl is a pale-yellow viscous oil, which usually solidifies on standing at 0 °C.[18] The coproportionation product was used without further purification. ^{31}P NMR showed 3 peaks corresponding to the (iPr$_2$P)C$_6$H$_4$)$_3$Sb (8.26 ppm), (iPr$_2$P)C$_6$H$_4$)$_2$SbCl (5.70 ppm, major peak), and (iPr$_2$P)C$_6$H$_4$)SbCl$_2$ (0.25 ppm). (see Supporting Information)

Synthesis of 1. To a suspension of [(tht)AuCl] (27.4 mg, 0.086 mmol) in THF (2 mL) was added a solution of (*o*-(iPr$_2$P)C$_6$H$_4$)$_2$PhSb (50 mg, 0.086 mmol) in THF (2 mL) at room temperature. After subsequent stirring for 10 min, volatiles were removed, and the residue was washed with pentane (10 mL). Removal of the residual solvent afforded **1** (55 mg, 79% yield) as a white powder. X-ray quality crystals were obtained by slow diffusion of pentane into a solution of the compound in THF. ^{1}H NMR (499.43 MHz; $CDCl_3$): δ 7.92 (d, 2H, *o*-P(Sb)C$_6$H$_4$, $^3J_{H-H}$ = 7.50 Hz), 7.48 (br, 2H, *o*-P(Sb)C$_6$H$_4$), 7.37 (pseudo-t, 4H, *o*-P(Sb)C$_6$H$_4$, $^3J_{H-H}$ = 7.50 Hz), 7.30 (m, 5H, SbPh−C*H*), 2.84 (m, 4H, C*H*CH$_3$), 1.50 (dd, 6H, $^3J_{H-H}$ = 7.50 Hz, $^3J_{H-P}$ = 19.50 Hz, CHC*H*$_3$), 1.42 (dd, 6H, $^3J_{H-H}$ = 7.50 Hz, $^3J_{H-P}$ = 19.50 Hz, CHC*H*$_3$), 1.24 (dd, 6H, $^3J_{H-H}$ = 7.20 Hz, $^3J_{H-P}$ = 15.0 Hz, CHC*H*$_3$), 0.91 (dd, 6H, $^3J_{H-H}$ = 7.20 Hz, $^3J_{H-P}$ = 19.50 Hz, CHC*H*$_3$). ^{13}C{^{1}H} NMR (125.58 MHz; $CDCl_3$): δ 150.34 (t, J_{C-P} = 16.32 Hz), 145.34 (t, J_{C-P} = 11.90 Hz), 137.06 (t, J_{C-P} = 6.81 Hz), 136.01 (s), 135.26 (t, J_{C-P} = 21.31 Hz), 131.97 (br), 131.02 (s), 129.05 (s), 128.67 (t, J_{C-P} = 3.12 Hz), 128.10 (s), 26.04 (pseudo-t, J_{C-P} = 15.12 Hz, *C*(CH$_3$)$_2$), 24.13 (pseudo-t, J_{C-P} = 12.65 Hz, *C*(CH$_3$)$_2$), 20.53 (s, CH$_{3i\text{-}Pr}$), 19.61 (s, CH$_{3i\text{-}Pr}$), 19.53 (s, CH$_{3i\text{-}Pr}$), 16.68 (s, CH$_{3i\text{-}Pr}$). ^{31}P{^{1}H} NMR (202.17 MHz; $CDCl_3$): δ 69.18. Elemental analysis calculated (%) for $C_{30}H_{41}AuClP_2Sb$: C, 44.06; H, 5.05. Found: C, 43.47; H, 5.15.

Synthesis of 2. (*o*-(iPr$_2$P)C$_6$H$_4$)$_2$SbCl (232.5 mg, 0.43 mmol) was prepared by stirring (*o*-(iPr$_2$P)C$_6$H$_4$)$_3$Sb (200.0 mg, 0.29 mmol) and

dx.doi.org/10.1021/ic400736b | Inorg. Chem. 2013, 52, 7145−7151

$SbCl_3$ (32.5 mg, 0.14 mmol) for 3 h at 90 °C under neat conditions. Then, the suspension of [(tht)AuCl] (137.8 mg, 0.43 mmol) in THF (5 mL) was slowly added a solution of $(o\text{-}(i\text{Pr}_2\text{P})C_6H_4)_2SbCl$ in THF (15 mL) at room temperature. After subsequent stirring for 30 min, volatiles were removed, and the residue was washed with pentane (10 mL). Removal of the residual solvent afforded **2** (183.5 mg, 55% yield) as a yellow powder. X-ray quality crystals were obtained by slow diffusion of Et_2O into a solution of the compound in CH_2Cl_2. ^{1}H NMR (399.59 MHz; $CDCl_3$): δ 8.53 (d, 2H, *o*-P(Sb)C_6H_4, $^3J_{H-H}$ = 7.65 Hz), 7.61 (m, 2H, *m*-P(Sb)C_6H_4), 7.41 (br, 4H, *o*-P(Sb)C_6H_4 + *m*-P(Sb)C_6H_4), 3.05 (m, 2H, C*H*CH_3), 2.90 (m, 2H, C*H*CH_3), 1.59 (dd, 6H, $^3J_{H-H}$ = 8.25 Hz, $^3J_{H-P}$ = 18.55 Hz, CHC*H*$_3$), 1.37 (dd, 6H, $^3J_{H-H}$ = 8.25 Hz, $^3J_{H-P}$ = 18.55 Hz, CHC*H*$_3$), 1.27 (dd, 6H, $^3J_{H-H}$ = 8.25 Hz, $^3J_{H-P}$ = 18.55 Hz, CHC*H*$_3$), 0.94 (dd, 6H, $^3J_{H-H}$ = 8.25 Hz, $^3J_{H-P}$ = 18.55 Hz, CHC*H*$_3$). ^{13}C{^{1}H} NMR (125.58 MHz; $CDCl_3$): δ 152.69 (t, J_{C-P} = 18.09 Hz), 135.49 (t, J_{C-P} = 8.25 Hz), 133.33 (t, J_{C-P} = 24.74 Hz), 132.46 (s), 131.91 (s), 128.89 (s), 26.21 (pseudo-t, J_{C-P} = 14.11 Hz, $C(CH_3)_2$), 25.29 (pseudo-t, J_{C-P} = 14.11 Hz, $C(CH_3)_2$), 20.17 (s, $CH_{3i\text{-}Pr}$), 19.37 (s, $CH_{3i\text{-}Pr}$), 18.56 (s, $CH_{3i\text{-}Pr}$), 16.81 (s, $CH_{3i\text{-}Pr}$). ^{31}P{^{1}H} NMR (161.73 MHz; $CDCl_3$): δ 64.18. Elemental analysis calculated (%) for $C_{24}H_{36}AuCl_2P_2Sb$: C, 37.14; H, 4.68. Found: C, 37.08; H, 4.65.

Synthesis of 3. A THF solution (3 mL) of [(tht)AuCl] (56.0 mg, 0.16 mmol) was added dropwise to a THF solution (2 mL) of $(o\text{-}(i\text{Pr}_2\text{P})C_6H_4)_3Bi$ (70.0 mg, 0.08 mmol) at ambient temperature. The resulting mixture was allowed to stir for 12 h. The solvent was then removed under reduced pressure to give a light yellow solid, which was washed with pentane (3 × 5 mL) to remove the $[\{o\text{-}(i\text{Pr}_2\text{P})\text{-}C_6H_4Au\}_2]$ dimer complex. The resulting residue was dried under reduced pressure to afford a light yellow solid (46.1 mg, 61% yield). Fractional crystallization from CH_2Cl_2/Et_2O afforded yellow crystals of **3**. ^{1}H NMR (499.43 MHz; $CDCl_3$): δ 9.18 (d, 2H, *o*-P(Bi)C_6H_4, $^3J_{H-H}$ = 7.31 Hz), 7.88 (pseudo-t, 2H, *m*-P(Bi)C_6H_4, $^3J_{H-H}$ = 7.83 Hz), 7.57 (br, 2H, *m*-P(Bi)C_6H_4), 7.53 (pseudo-t, 2H, *m*-P(Bi)C_6H_4, $^3J_{H-H}$ = 7.83 Hz), 3.15 (m, 2H, C*H*CH_3), 2.91 (m, 2H, C*H*CH_3), 1.60 (dd, 6H, $^3J_{H-H}$ = 7.80 Hz, $^3J_{H-P}$ = 19.80 Hz, CHC*H*$_3$), 1.33 (dd, 6H, $^3J_{H-H}$ = 7.80 Hz, $^3J_{H-P}$ = 19.80 Hz, CHC*H*$_3$), 1.25 (dd, 6H, $^3J_{H-H}$ = 7.80 Hz, $^3J_{H-P}$ = 19.80 Hz, CHC*H*$_3$), 1.03 (dd, 6H, $^3J_{H-H}$ = 7.80 Hz, $^3J_{H-P}$ = 19.80 Hz, CHC*H*$_3$). ^{13}C{^{1}H} NMR (125.58 MHz; $CDCl_3$): δ 179.59 (t, J_{C-P} = 17.46 Hz), 138.09 (t, J_{C-P} = 8.68 Hz), 137.23 (t, J_{C-P} = 24.39 Hz), 136.05 (s), 135.52 (s), 127.93 (s), 26.15 (pseudo-t, J_{C-P} = 14.23 Hz, $C(CH_3)_2$), 25.33 (pseudo-t, J_{C-P} = 14.23 Hz, $C(CH_3)_2$), 20.66 (s, $CH_{3i\text{-}Pr}$), 19.54 (s, $CH_{3i\text{-}Pr}$), 18.78 (s, $CH_{3i\text{-}Pr}$), 17.01 (s, $CH_{3i\text{-}Pr}$). ^{31}P{^{1}H} NMR (202.16 MHz; $CDCl_3$): δ 57.05. Elemental analysis calculated (%) for $C_{24}H_{36}AuCl_2P_2Bi + Et_2O$: C, 35.87; H, 4.95. Found: C, 35.93; H, 4.58 (approx. 1 equiv of ether was lost in drying).

Synthesis of 5. A solution of *o*-chloranil (12.0 mg, 0.049 mmol) in CH_2Cl_2 (1 mL) was added dropwise to a solution of **1** (40.0 mg, 0.049 mmol) in CH_2Cl_2 (5 mL) at ambient temperature. The reaction was stirred for 10 min before removing the solvent in vacuo. The resulting yellow solid was washed with pentane (2 × 3 mL) and dried in vacuo to afford 42.1 mg (81%) of **5** as an orange powder. Single crystals of **5** suitable for X-ray diffraction were obtained by vapor diffusion of pentane into a solution of the compound in THF. ^{1}H NMR (499.43 MHz; $CDCl_3$): δ 8.34 (d, 2H, *o*-P(Sb)C_6H_4, $^3J_{H-H}$ = 8.00 Hz), 7.75 (d, 2H, *o*-P(Sb)C_6H_4, $^3J_{H-H}$ = 8.00 Hz), 7.56 (t, 2H, *m*-P(Sb)C_6H_4, $^3J_{H-H}$ = 8.00 Hz), 7.47 (t, 2H, *m*-P(Sb)C_6H_4, $^3J_{H-H}$ = 8.00 Hz), 7.11 (t, 1H, *p*-SbPhC*H*, $^3J_{H-H}$ = 7.50 Hz), 7.01 (t, 2H, *o*-SbPhC*H* or *m*-SbPhC*H*, $^3J_{H-H}$ = 7.50 Hz), 6.87 (d, 2H, *o*-SbPhC*H* or *m*-SbPhC*H*, $^3J_{H-H}$ = 7.50 Hz), 3.41 (m, 4H, C*H*CH_3), 1.41 (dd, 6H, $^3J_{H-H}$ = 7.50 Hz, $^3J_{H-P}$ = 19.00 Hz, CHC*H*$_3$), 1.31 (dd, 6H, $^3J_{H-H}$ = 7.50 Hz, $^3J_{H-P}$ = 17.50 Hz, CHC*H*$_3$), 1.19 (dd, 6H, $^3J_{H-H}$ = 7.50 Hz, $^3J_{H-P}$ = 19.00 Hz, CHC*H*$_3$), 1.12 (dd, 6H, $^3J_{H-H}$ = 7.50 Hz, $^3J_{H-P}$ = 17.50 Hz, CHC*H*$_3$). ^{13}C{^{1}H} NMR (125.58 MHz; $CDCl_3$): δ 167.69 (t, J_{C-P} = 28.88 Hz), 151.03 (s), 149.08 (s), 146.43 (s), 135.53 (t, J_{C-P} = 10.93 Hz), 133.92 (s), 133.23 (s), 131.54 (t, J_{C-P} = 5.78 Hz), 129.31 (s), 129.09 (t, J_{C-P} = 3.52 Hz), 128.13 (s), 120.19 (s), 119.96 (s, $O_2C_6Cl_4$), 119.73 (s, $O_2C_6Cl_4$), 119.53 (s, $O_2C_6Cl_4$), 117.75 (s, $O_2C_6Cl_4$), 117.03 (s, $O_2C_6Cl_4$), 116.43 (s, $O_2C_6Cl_4$), 28.93 (pseudo-t, J_{C-P} = 13.81 Hz), 27.39 (pseudo-t, J_{C-P} = 13.81 Hz), 19.34 (s), 19.19 (s), 18.99 (s), 18.70 (s). ^{31}P{^{1}H} NMR (202.17 MHz; $CDCl_3$): δ 103.26. Elemental analysis calculated (%) for $C_{36}H_{41}AuCl_5O_2P_2Sb$: C, 40.65; H, 3.89. Found: C, 39.04; H, 3.81.

Synthesis of 6. A solution of *o*-chloranil (15.8 mg, 0.064 mmol) in CH_2Cl_2 (1 mL) was added dropwise to a solution of **2** (50.0 mg, 0.064 mmol) in CH_2Cl_2 (5 mL) at ambient temperature. The reaction was stirred for 10 min before removing the solvent in vacuo. The resulting yellow solid was washed with pentane (2 × 3 mL) and dried in vacuo to afford 57.5 mg (88%) of **6** as an orange powder. ^{1}H NMR (499.43 MHz; $CDCl_3$): δ 8.69 (d, 2H, *o*-P(Sb)C_6H_4, $^3J_{H-H}$ = 8.20 Hz), 7.72 (m, 4H), 7.52 (t, 2H, *m*-P(Sb)C_6H_4, $^3J_{H-H}$ = 8.20 Hz), 3.44 (m, 4H, C*H*CH_3), 1.42 (m, 12H, CHC*H*$_3$), 1.35 (dd, 6H, $^3J_{H-H}$ = 8.36 Hz, $^3J_{H-P}$ = 19.03 Hz, CHC*H*$_3$), 1.25 (dd, 6H, $^3J_{H-H}$ = 8.36 Hz, $^3J_{H-P}$ = 19.03 Hz, CHC*H*$_3$). ^{13}C{^{1}H} NMR (125.58 MHz; $CDCl_3$): δ 147.18 (s), 146.71 (s), 134.89 (s), 134.16 (t, J_{C-P} = 10.34 Hz), 130.50 (t, J_{C-P} = 5.48 Hz), 130.22 (s), 119.83 (s, $O_2C_6Cl_4$), 119.64 (s, $O_2C_6Cl_4$), 118.40 (s, $O_2C_6Cl_4$), 117.13 (s, $O_2C_6Cl_4$), 115.13 (s, $O_2C_6Cl_4$), 114.88 (s, $O_2C_6Cl_4$), 28.77 (pseudo-t, J_{C-P} = 15.10 Hz, $C(CH_3)_2$), 27.95 (pseudo-t, J_{C-P} = 13.55 Hz, $C(CH_3)_2$), 19.09 (s, $CH_{3i\text{-}Pr}$), 19.02 (s, $CH_{3i\text{-}Pr}$), 18.96 (s, $CH_{3i\text{-}Pr}$), 18.65 (s, $CH_{3i\text{-}Pr}$). ^{31}P{^{1}H} NMR (202.17 MHz; $CDCl_3$): δ 108.63. Elemental analysis calculated (%) for $C_{30}H_{36}AuCl_6O_2P_2Sb$ + 0.6 THF: C, 36.53; H, 3.86. Found: C, 36.69; H, 3.92 (approximately 0.6 equiv of THF was lost in drying, see Supporting Information).

Crystallography. All crystallographic measurements were performed at 110(2) K using a Bruker SMART APEX II diffractometer with a CCD area detector (graphite monochromated Mo K_α radiation, λ = 0.71073 Å) at 110 K. In each case, a specimen of suitable size and quality was selected and mounted onto a nylon loop. The semiempirical method SADABS was applied for absorption correction. The structures were solved by direct methods and refined by the full-matrix least-squares technique against F^2 with the anisotropic temperature parameters for all non-hydrogen atoms. All H atoms were geometrically placed and refined in riding model approximation. Data reduction and further calculations were performed using the Bruker SAINT+ and SHELXTL NT program packages.[19]

Theoretical Calculations. Density functional theory (DFT) calculations (full geometry optimization) were carried out on **1**, **2**, **3**, **4**, **5**, and **6** starting from the crystal structure geometries with the Gaussian09[20] program (BP86[21] with 6-31g for H, C, O; Stuttgart relativistic small core (RSC) 1997 ECP for Au;[22] Stuttgart relativistic large core (RLC) 1997 ECP for P,[23] Cl, Sb,[24] Bi).[25] Frequency calculations were also carried out on the optimized geometry, showing no imaginary frequencies. The optimized structures, which are in excellent agreement with the solid-state structures, were subjected to a NBO analysis.[26] The resulting Natural Localized Molecular Orbitals (NLMOs) were visualized and plotted in Jimp 2 program.[27]

■ ASSOCIATED CONTENT

Supporting Information

Additional experimental and computational details. Crystallographic data in cif format. This material is available free of charge via the Internet at http://pubs.acs.org.

■ AUTHOR INFORMATION

Corresponding Author

*E-mail: francois@tamu.edu.

Notes

The authors declare no competing financial interest.

■ ACKNOWLEDGMENTS

This work was supported by the National Science Foundation (CHE-0952912 and CHE-1300371), the Welch Foundation (A-1423), and Texas A&M University (Davidson Professorship).

REFERENCES

(1) (a) Champness, N. R.; Levason, W. *Coord. Chem. Rev.* **1994**, *133*, 115−217. (b) Jimenez-Tenorio, M.; Puerta, M. C.; Salcedo, I.; Valerga, P.; Rios, I. D.; Mereiter, K. *Dalton Trans.* **2009**, 1842−1852. (c) Levason, W.; Reid, G. *Coord. Chem. Rev.* **2006**, *250*, 2565−2594. (d) Levason, W.; McAuliffe, C. A. *Acc. Chem. Res.* **1978**, *11*, 363−368. (e) Werner, H. *Angew. Chem., Int. Ed.* **2004**, *43*, 938−954.

(2) Wade, C. R.; Gabbaï, F. P. *Angew. Chem., Int. Ed.* **2011**, *50*, 7369−7372.

(3) (a) Parkin, G. *Organometallics* **2006**, *25*, 4744−4747. (b) Hill, A. F. *Organometallics* **2006**, *25*, 4741−4743. (c) Fontaine, F. G.; Boudreau, J.; Thibault, M. H. *Eur. J. Inorg. Chem.* **2008**, 5439−5454. (d) Braunschweig, H.; Dewhurst, R. D.; Schneider, A. *Chem. Rev.* **2010**, *110*, 3924−3957. (e) Bouhadir, G.; Amgoune, A.; Bourissou, D. *Adv. Organomet. Chem.* **2010**, *58*, 1−107. (f) Amgoune, A.; Bourissou, D. *Chem. Commun.* **2011**, *47*, 859−871. (g) Braunschweig, H.; Dewhurst, R. D. *Dalton Trans.* **2011**, *40*, 549−558. (h) Rudd, P. A.; Liu, S.; Gagliardi, L.; Young, V. G.; Lu, C. C. *J. Am. Chem. Soc.* **2011**, *133*, 20724−20727. (i) Bauer, J.; Braunschweig, H.; Dewhurst, R. D. *Chem. Rev.* **2012**, *112*, 4329−4346. (j) Anderson, J. S.; Moret, M.-E.; Peters, J. C. *J. Am. Chem. Soc.* **2013**, *135*, 534−537.

(4) (a) Lin, T.-P.; Wade, C. R.; Pérez, L. M.; Gabbaï, F. P. *Angew. Chem., Int. Ed.* **2010**, *49*, 6357−6360. (b) Wade, C. R.; Lin, T.-P.; Nelson, R. C.; Mader, E. A.; Miller, J. T.; Gabbaï, F. P. *J. Am. Chem. Soc.* **2011**, *133*, 8948−8955. (c) Wade, C. R.; Ke, I.-S.; Gabbaï, F. P. *Angew. Chem., Int. Ed.* **2012**, *51*, 478−481. (d) Lin, T.-P.; Nelson, R. C.; Wu, T.; Miller, J. T.; Gabbaï, F. P. *Chem. Sci.* **2012**, *3*, 1128−1136.

(5) (a) Ohkata, K.; Takemoto, S.; Ohnishi, M.; Akiba, K.-y. *Tetrahedron Lett.* **1989**, *30*, 4841−4844. (b) Yi, W.; Tan, N. *Acta Crystallogr., Sect. E: Struct. Rep. Online* **2011**, *67*, m917.

(6) Benjamin, S. L.; Levason, W.; Reid, G.; Warr, R. P. *Organometallics* **2012**, *31*, 1025−1034.

(7) (a) Tschersich, C.; Limberg, C.; Roggan, S.; Herwig, C.; Ernsting, N.; Kovalenko, S.; Mebs, S. *Angew. Chem., Int. Ed.* **2012**, *51*, 4989−4992. (b) Lin, T.-P.; Ke, I.-S.; Gabbaï, F. P. *Angew. Chem., Int. Ed.* **2012**, *51*, 4985−4988.

(8) (a) Cordero, B.; Gomez, V.; Platero-Prats, A. E.; Reves, M.; Echeverria, J.; Cremades, E.; Barragan, F.; Alvarez, S. *Dalton Trans.* **2008**, 2832−2838. (b) Pyykkö, P.; Atsumi, M. *Chem.—Eur. J.* **2009**, *15*, 186−197.

(9) Jones, P. G. *Acta Crystallogr., Sect. C: Cryst. Struct. Commun.* **1992**, *48*, 1487−1488.

(10) Becker, G.; Mundt, O.; Sachs, M.; Breunig, H. J.; Lork, E.; Probst, J.; Silvestru, A. *Z. Anorg. Allg. Chem.* **2001**, *627*, 699−714.

(11) Hall, M.; Sowerby, D. B. *J. Organomet. Chem.* **1988**, *347*, 59−70.

(12) Milićcev, S.; Hadzi, D. *Inorg. Chim. Acta* **1977**, *21*, 201−207.

(13) Sircoglou, M.; Bontemps, S.; Mercy, M.; Saffon, N.; Takahashi, M.; Bouhadir, G.; Maron, L.; Bourissou, D. *Angew. Chem., Int. Ed.* **2007**, *46*, 8583−8586.

(14) N. Gibbons, M.; J. Begley, M.; J. Blake, A.; Bryan Sowerby, D. *J. Chem. Soc., Dalton Trans.* **1997**, 2419−2426.

(15) The notion of valence refers to the number of electrons that an atom involves in bonding. Here, the structure of **5** suggests that the gold atom involves three of its valence electron in bonding. Additional clarification on the notion of valence is provided in the following reference. Parkin, G. *J. Chem. Educ.* **2006**, *83*, 791−799.

(16) Uson, R.; Laguna, A.; Laguna, M. *Inorg. Synth.* **1989**, *26*, 85−91.

(17) Korshin, E. E.; Leitus, G.; Shimon, L. J. W.; Konstantinovski, L.; Milstein, D. *Inorg. Chem.* **2008**, *47*, 7177−7189.

(18) (a) Chan, K. H.; Leong, W. K.; Mak, K. H. G. *Organometallics* **2006**, *25*, 250−259. (b) Nunn, M.; Sowerby, D. B.; Wesolek, D. M. *J. Organomet. Chem.* **1983**, *251*, C45−C46.

(19) (a) *SAINTPlus, Data Reduction and Correction Program*, v. 6.2; Bruker AXS: Madison, WI, 2001. (b) Sheldrick, G. M. *SHELXTL*, Version 6.1; Bruker Analytical X-ray Systems, Inc.: Madison, WI.

(20) Frisch, M. J.; Trucks, G. W.; Schlegel, H. B.; Scuseria, G. E.; Robb, M. A.; Cheeseman, J. R.; Scalmani, G.; Barone, V.; Mennucci, B.; Petersson, G. A.; Nakatsuji, H.; Caricato, M.; Li, X.; Hratchian, H. P.; Izmaylov, A. F.; Bloino, J.; Zheng, G.; Sonnenberg, J. L.; Hada, M.; Ehara, M.; Toyota, K.; Fukuda, R.; Hasegawa, J.; Ishida, M.; Nakajima, T.; Honda, Y.; Kitao, O.; Nakai, H.; Vreven, T.; Montgomery, J., J. A.; Peralta, J. E.; Ogliaro, F.; Bearpark, M.; Heyd, J. J.; Brothers, E.; Kudin, K. N.; Staroverov, V. N.; Kobayashi, R.; Normand, J.; Raghavachari, K.; Rendell, A.; Burant, J. C.; Iyengar, S. S.; Tomasi, J.; Cossi, M.; Rega, N.; Millam, J. M.; Klene, M.; Knox, J. E.; Cross, J. B.; Bakken, V.; Adamo, C.; Jaramillo, J.; Gomperts, R.; Stratmann, R. E.; Yazyev, O.; Austin, A. J.; Cammi, R.; Pomelli, C.; Ochterski, J. W.; Martin, R. L.; Morokuma, K.; Zakrzewski, V. G.; Voth, G. A.; Salvador, P.; Dannenberg, J. J.; Dapprich, S.; Daniels, A. D.; Farkas, Ö.; Foresman, J. B.; Ortiz, J. V.; Cioslowski, J.; Fox, D. J. *Gaussian 09*, Revision B.01; Gaussian, Inc.: Wallingford, CT, 2009.

(21) (a) Becke, A. D. *Phys. Rev. A* **1988**, *38*, 3098−3100. (b) Perdew, J. P. *Phys. Rev. B* **1986**, *33*, 8822−8824.

(22) Figgen, D.; Rauhut, G.; Dolg, M.; Stoll, H. *Chem. Phys.* **2005**, *311*, 227−244.

(23) Bergner, A.; Dolg, M.; Küchle, W.; Stoll, H.; Preuß, H. *Mol. Phys.* **1993**, *80*, 1431−1441.

(24) Metz, B.; Stoll, H.; Dolg, M. *J. Chem. Phys.* **2000**, *113*, 2563−2569.

(25) Stoll, H.; Metz, B.; Dolg, M. *J. Comput. Chem.* **2002**, *23*, 767−778.

(26) Glendening, E. D.; Badenhoop, J. K.; Reed, A. E.; Carpenter, J. E.; Bohmann, J. A.; Morales, C. M.; Weinhold, F. *NBO 5.9*; Theoretical Chemistry Institute, University of Wisconsin: Madison, WI, 2011.

(27) Manson, J.; Webster, C. E.; Pérez, L. M.; Hall, M. B., http://www.chem.tamu.edu/jimp2/index.html.